MAPA: a New High-precision 3D Method of Palatal Miniscrew Placement

Giuliano Maino
Department of Orthodontics,
University of Ferrara, Ferrara, Italy

Emanuele Paoletto
Orthodontic Technician,
Thiene (VI), Italy

Luca Lombardo
Department of Orthodontics,
University of Ferrara, Ferrara, Italy

Giuseppe Siciliani
Department of Orthodontics,
University of Ferrara, Ferrara, Italy

Correspondence:
e-mail: lulombardo@tiscali.it

Article history:
Received: 29/06/2014
Accepted: 06/02/2015
Published online:20/05/2015

Conflict of interest:
The authors declare that they have no conflicts of interest related to this research.

How to cite this article:
Maino G, Paoletto E, Lombardo L, Siciliani G. MAPA: a new high-precision 3D method of palatal miniscrew placement. *EJCO* 2015;**3**:41-47

This article describes a new insertion guide system that facilitates the precise directional positioning of miniscrews on the palate. The MAPA (MAino-PAoletto) guide is made with the aid of cone-beam computed tomography (CBCT) images and digital casts. The development of purpose-designed software has enabled the design and construction of insertion guides that allow good exploitation of available bone, making miniscrews placement safer and more precise.
The application of this method to a clinical case is discussed, as well as the indications, efficacy and possible complications of the device.

Keywords
Digital printing, miniscrew, mini-implant, stent, template, insertion guide, stereolithographic guide, palatal miniscrew insertion guide, Class III

doi:10.12889/2015_C00239

INTRODUCTION

Insertion of miniscrews for orthodontic anchorage into the palatal vault is finding ever more applications in the field of dentistry[1–5]. This anchorage site is useful for both biomechanical and, especially, anatomical reasons, as there are no roots that could interfere with miniscrew insertion[6–8]. Nevertheless, the palate does not present a uniform thickness, varying from individual to individual[9,10], and great care therefore needs to be taken to analyze the availability of bone to guarantee good primary stability and reliable anchorage[11,12].

In recent years, volumetric tomography and purpose-designed software have enabled the design and construction of templates that allow good exploitation of the available bone, making miniscrew placement safer and more precise[13]. These 3D guides are generally constructed for miniscrew placement in the inter-radicular spaces, specifically to prevent any damage to tooth roots[14–16]. However, we present here a miniscrew insertion guide designed specifically for palatal application. This template is able to ensure not only miniscrews are placed at the correct depth in the maxillary bone, but also that multiple implants are parallel. It is therefore suitable for miniscrews destined for the anchorage of removable devices, as well as pre-formed and tailored appliances used in fixed orthodontics.

MATERIALS AND METHODS

Identification of miniscrew insertion sites

In order to correctly position miniscrews in the palate and guarantee that they are parallel, it is essential to perform a thorough evaluation of the maxillary bone structure. The most precise imaging technique in this regard is cone-beam computed tomography (CBCT), which should be performed with the mouth lightly open. In order to ensure that the occlusal surfaces do not overlap, and that the patient can maintain the correct position during the scan, a roll of cotton wool should be placed between the patient's teeth *(Fig. 1)* (KaVo 3D eXam). A DICOM file of the image is generated that should enable identification of the anatomical structures in the roof of the palate, and thereby the most suitable sites for miniscrew insertion. Should the use of CBCT merely for miniscrew placement be considered too risky for the patients, exposing them to a relatively large amount of radiation[17], it is possible to use teleradiography instead. Indeed, according to Kim et al., palatal thicknesses measured via laterolateral teleradiography are comparable to those measured on CBCT scans taken roughly 5 mm from the midsagittal plane[18]. Nevertheless, teleradiography must not be performed without intraoral positioning of a thermoplastic PET-G bite, cast on the patient's plaster model, featuring a series of radio-opaque markers along the medial palatine raphe *(Fig. 2)*. This will enable precise reconstruction of the profile of the palatal mucosa on the scanned image (after factoring in the magnification of the scanning device itself).

Contemporaneously, on an STL file obtained by scanning the stone model (3shape D800 scanner) or the impression of the patient's upper arch, two ideal miniscrews insertion points (IIPs) are identified in the anterior portion of the palate, preferably in an area between the distal surfaces of the canines and the mesial surfaces of the second premolars *(Fig. 3)*, bearing in mind that the ideal distance between the two is, in most cases, 10 mm.

Next, the digital model of the upper arch is superimposed onto the DICOM file *(Fig. 4)* or the lateral x-ray *(Fig. 5)*, enabling identification of the most suitable anteroposterior placement, based on the width and thickness of the palatal vault. This operation is performed using a proprietary software method (eXam Vision software integrated with Rhinoceros software).

Next, by means of STL files, miniscrews are virtually 'inserted' *(Fig. 6)* into the palate. By varying the position of the virtual implant, the miniscrew of greatest length compatible with the patient's anatomy can be selected on

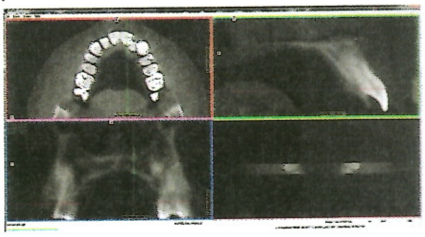

Figure 1: DICOM file of the cone-beam computed tomography (CBCT) scan.

Figure 2: X-ray and lateral cephalogram showing radio-opaque markers along the medial palatine raphe.

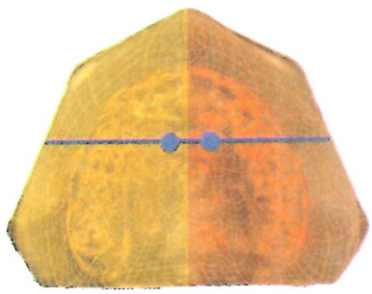

Figure 3: STL model and ideal miniscrew insertion point (IIPS).

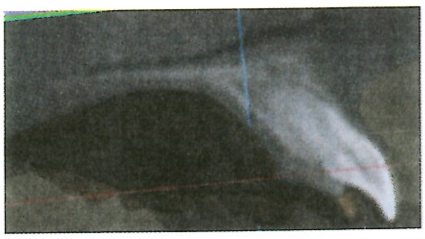

Figure 4: Superimposition of the digital model on CBCT.

doi:10.12889/2015_C00239

the basis of the availability of bone. Modification of the virtual miniscrew angle and insertion points should enable the identification of sites with sufficient bone to allow application of miniscrews of at least 9 mm in length. In order to better exploit the available bone, miniscrews (Spider Screw Regular Plus) should be inserted with an anterior inclination *(Fig. 6)*[19], at an angle compatible with the bands that will be welded to the device[20]. At this point, it would be opportune to check the overall plan in 3D to ensure that the miniscrew length is suitable and that the programmed placement is parallel *(Fig. 7)*.

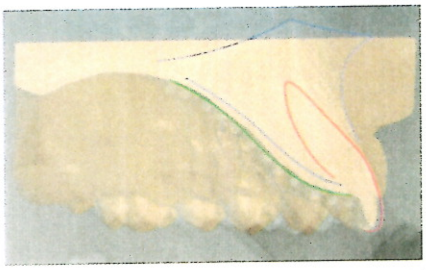

Figure 5: Superimposition of the digital model on the lateral cephalogram.

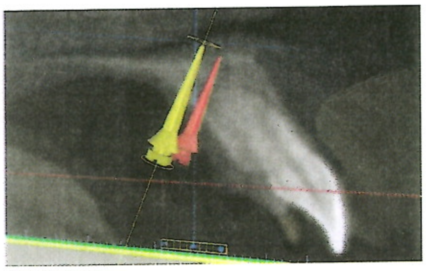

Figure 6: STL files showing an inserted miniscrew on the sagittal plane of the cone-beam computed tomography (CBCT) scan passing through the ideal insertion point.

Figure 7: Checking the inclination between the axis of the miniscrew and the axis of the molars.

Template design

The insertion guide is designed to rest upon the occlusal surfaces of the posterior teeth *(Fig. 8)* and act as a precise guide to the insertion site, specifically its location, depth and the direction of miniscrew application. It must be stable, and permit good visibility and easy removal once the miniscrews are in place. The use of STL images of the miniscrews and pick-up driver during the design phase enables the faithful reproduction of their measurements, in particular the transmucosal portion of the miniscrews and the insertion device *(Fig. 9)*. These measurements will be transferred to the internal part of the two cylindrical guides designed to replicate the angle of insertion and prevent the screws from penetrating beyond the required depth. The cylindrical guides are virtually joined to the template by means of resin bridges *(Fig. 10)*. The guide is then 3D-printed in a transparent material (DWS 3D printer Digital Wax 020), to ensure maximum visibility during the insertion procedure, and that the resin bridges can be easily detached from the body of the guide and subsequently removed *(Fig. 11)*. Insertion will be facilitated by a 'window' in each cylinder, purpose-designed to enable the orthodontist to check the progress of the operation and ensure that the miniscrew has reached the programmed depth.

Miniscrew application

After local anaesthesia to the palatal site (2% lidocaine), the surgical guide is fitted, making sure that it rests on the occlusal surfaces of the posterior teeth. If required, a small amount of light-cure resin (Triad; Dentsply, York, Pennsylvania, USA) can be used to bond the template to the occlusal surfaces of the first premolars.

Two self-tapping, self-drilling miniscrews (Spider Screw Regular Plus) capable of accepting an abutment fixed with a microscrew *(Fig. 12)* are selected, picked up with the specific driver - mounted on a low-speed contra-angle handpiece

Figure 8: The template resting on the occlusal surface of the posterior teeth.

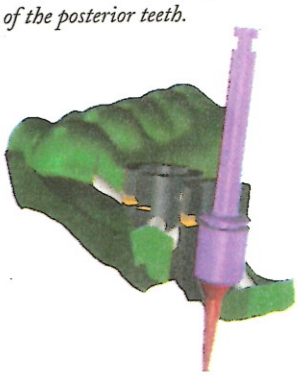

Figure 9: Section of the insertion guide showing the STL files of the miniscrew and pick-up driver.

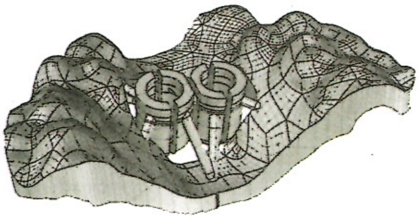

Figure 10: Connection bridges between the cylindrical guide and the template body.

(50 rpm) - and by these means inserted into the apposite guide cylinder of the template. The design of the clear cylinder will ensure that the screw is inserted at the right angle and to the required depth. Indeed, the guide is able to replicate with extreme precision the transmucosal portion of the miniscrew and driver, and can prevent the screw exceeding the pre-programmed depth. The horizontal viewing window in each cylinder is positioned at exactly the height of the pick-up driver head, providing the operator with a direct view of the insertion progress, and blocking the driving action when the upper margin of the pick-up driver reaches the

doi:10.12889/2015_C00239

Figure 11: Cylindrical guide removal after miniscrew insertion.

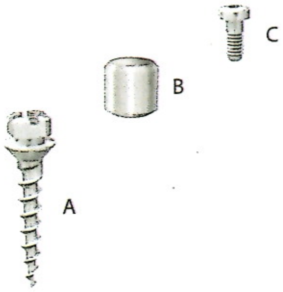

Figure 12: Hybrid rapid palatal expander (RPE) components: (A) Spider Screw Regular Plus, (B) abutment, (C) fixation screw

Figure 13: Bands on first molars and pick-up coping in place for the polyvinyl siloxane (PVS) impression.

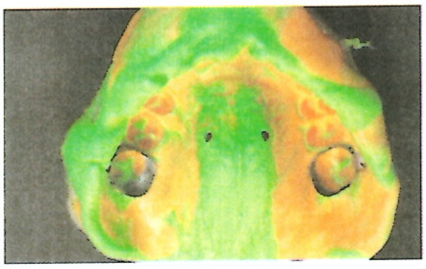

Figure 14: Polyvinyl siloxane (PVS) impression.

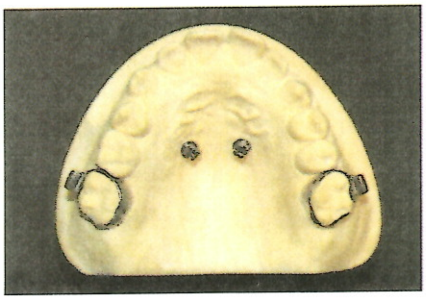

Figure 15: Stone model.

lower margin of the viewing window. Once the miniscrews are in place, the resin bridges connecting the cylinders from the body of the guide can be cut *(Fig. 11)*, and the resulting sections of the template can easily be removed.

Construction of the orthodontic device

At this point, the anchorage bands can be fitted onto the first molars. Two plastic transfer copings *(Fig. 13)* are then simply clicked onto the heads of the miniscrews, and a plastic tray is used to take a silicon or vinyl polysiloxane precision impression *(Fig. 14)* so that the position of the miniscrews can be replicated on the plaster models *(Fig. 15)*. The orthodontic device SKAR III (Skeletal Alt-RAMEC for Class III) applied in this case is a rapid palatal expander (RPE), with mixed dental/skeletal anchorage, featuring welded vestibular arms to hold a face-mask *(Fig. 16)*. Two metal abutments designed to fit over the heads of the miniscrews (Spider Screw Regular Plus) are welded on the anterior metal arms of the RPE, and each is fixed in place by means of a microscrew fitted with an appropriate driver.

CASE REPORT

Diagnosis

An 8-year-old male patient attended a consultation, seeking treatment for anterior crossbite. Facial analysis revealed labial incompetence, slight mandibular protrusion, and maxillary retrusion, which was particularly evident when the patient smiled *(Figs. 17 and 18)*. Intraoral examination revealed healthy periodontal tissues, upper jaw constriction, and anterior and posterior crossbite *(Figs. 19–24)*. Occlusion was severe dental Class III on both sides *(Figs. 20 and 21)*. A panoramic radiograph *(Fig. 25)* showed the patient to be in mixed dentition. A cranial laterolateral teleradiograph *(Fig. 26)* and associated cephalometric tracing *(Fig. 27)* confirmed severe skeletal Class III, lower incisor lingual inclination and hypodivergence *(Table 1)*.

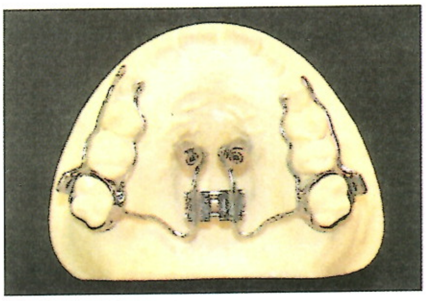

Figure 16: SKAR III (Skeletal Alt-RAMEC for Class III malocclusion).


Figures 17 and 18: Pre-treatment extraoral photos of the 8-year-old patient with skeletal Class III malocclusion.

Treatment objectives and treatment planning

The main objective of treatment was to expand and advance the upper jaw, minimizing the dental effects so as to obviate the need for subsequent compensatory measures. Hence we elected to use an RPE with mixed dental/skeletal anchorage, followed by a facial mask.

Treatment progress

Bands were positioned on the upper second deciduous molars and two 9 mm Spider Screw Regular Plus miniscrews inserted into the palate at the level of the first deciduous molars *(Fig. 28)*. The transfer copings were inserted by pressing on the miniscrews, and polyvinyl siloxane (PVS) precision impressions were taken. At this point a SKAR III appliance was constructed and anchored to the molar bands. Two vestibular arms were soldered onto the buccal side of the bands to be used for maxillary elastics, and two lingual arms were soldered onto the lingual aspect to distribute the force to the canine and first deciduous molars *(Fig. 29)*. Skeletal anchorage was provided by screwing metal abutments to the miniscrews fixed in the palate.

doi:10.12889/2015_C00239

Figures 19–24: Pre-treatment intraoral photos of the 8-year-old patient with skeletal Class III malocclusion.

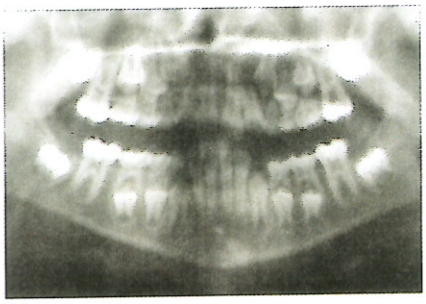

Figure 25: Panoramic radiograph.

Figure 26: Lateral cephalogram.

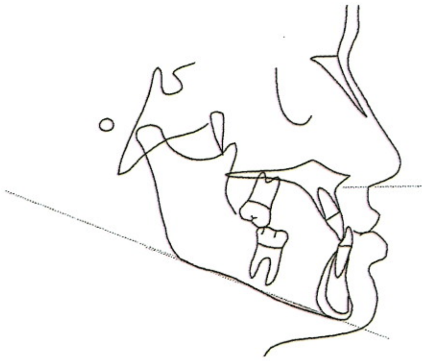

Figure 27: Pre-treatment tracing.

Figure 28: Two Spider Screw Regular Plus miniscrews inserted into the palate.

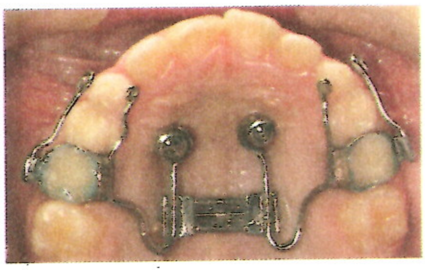

Figure 29: SKAR III appliance.

Figures 30–32: Intraoral photos after Liou's Alt-RAMEC protocol.

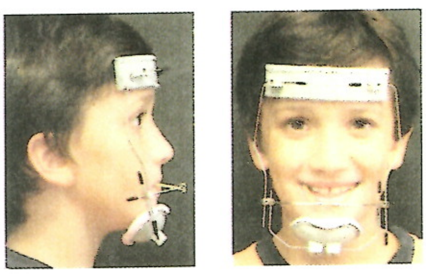

Figures 33 and 34: Starting the face mask.

Figures 35 and 36: Extraoral photos after 6 months of face-mask treatment .

Liou's protocol[21,22] was followed to bring about the maxillary expansion and mobilization, with the aim of achieving the required amount of occlusal overcorrection *(Figs. 30–32)*.
The expansion phase was followed by the use of the face-mask: 4 months worn 14 h per day *(Figs. 33 and 34)* and 7 months worn only during the night, which brought

doi:10.12889/2015_C00239

Measurements	Pre-treatment	Post-treatment
SNA	81	85
SNB	80.5	81
ANB	-0.5	4
WITS	-5	0
IMPA	79	77
SN-GoGn	37	37

Table 1: Cephalometric values (degrees).

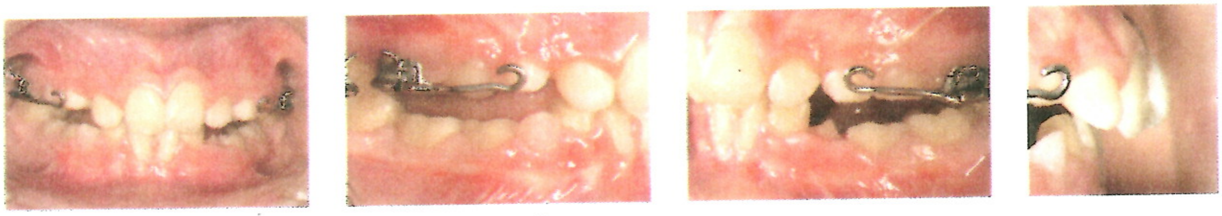

Figures 37–40: Intraoral photos after 6 months of face-mask treatment.

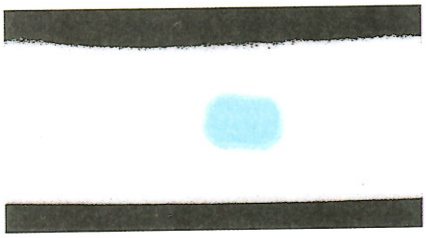

Figure 41: Microsensor embedded into the sponge of the support front.

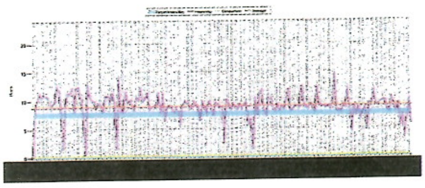

Figure 42: Graphic with wearing information for the face mask during the last 5 months of treatment.

about a considerable improvement in the sagittal relationship *(Figs. 35–40)*. Compliance was verified by a removable orthodontic appliance called TheraMon. The TheraMon chip offers more advantages xas a result of its smaller size (9x13 mm) and its increased accuracy and reliability[23-26]. A microsensor was embedded into the sponge of the support front *(Fig. 41)* and identified temperature changes, which are then transformed to wear time information *(Fig. 42)*. Indeed, radiography *(Fig. 43)* and cephalometric tracing *(Fig. 44)* show a large increase in upper jaw prominence, i.e. a 3.6° increase in the SNA angle, an increase of 7.5° in the ANB angle, a Wits index reduced to zero, slight lingual inclination of the lower incisors, and an increase in the divergency *(Table 1)*. Complete superimposition on the cranial base shows the forward and downward growth of the maxilla associated with the greater prominence of the upper jaw, while changes in the lower jaw appear to be negligible *(Fig. 45)*.

TREATMENT RESULT

After 12 months of treatment, the extraoral photos show the improved lip profile and the greater prominence of the upper jaw at the middle third of the face *(Fig. 36)*. The occlusal view *(Figs. 37–40)* shows how expansion has changed the shape of the arch, increasing the space available for the right upper canine.

DISCUSSION AND CONCLUSIONS

Skeletal anchorage has opened new frontiers in orthodontic treatment, and enabled the development of new techniques that provide good quality, predictable results[1-5]. The success of miniscrew techniques, such as that used here, depends upon the availability of supporting bone, and the use of miniscrews whose length and diameter allow the best use to be made of this support for anchorage. Cutting-edge imaging techniques such as CBCT and digital laser

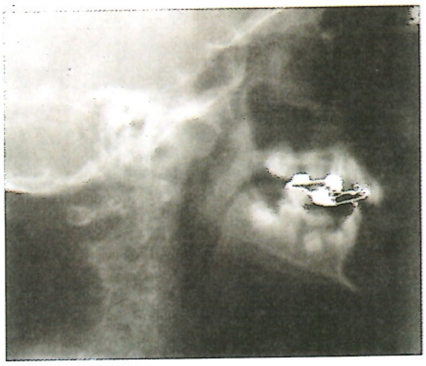

Figure 43: Post-treatment lateral cephalometry.

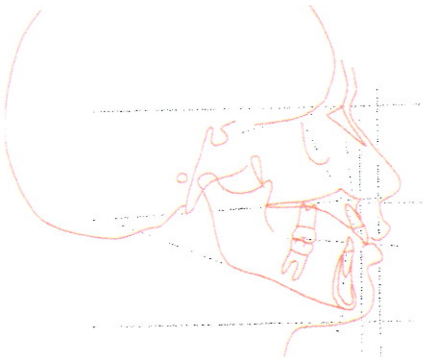

Figure 44: Post-treatment tracing.

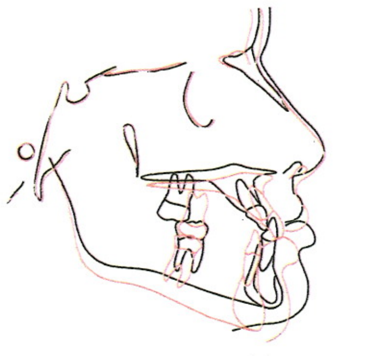

Figure 45: Complete superimposition.

doi:10.12889/2015_C00239

scanning have also fuelled great leaps forward, and combining these with 3D printing has enabled the construction of tailored surgical guides that facilitate the precise directional positioning of miniscrews. This approach optimizes and improves the safety of miniscrew placement, which can be inserted at the correct angle to the correct depth even by relatively inexperienced dental surgeons[13-15]. Indeed, surgical guides like the one presented here make miniscrew insertion a simple, reproducible and reliable procedure, and the construction of such orthodontic aids is likely to become even more precise and less complicated as the technology advances. This will undoubtedly enable the orthodontist to achieve more predictable results within a reasonable, and perhaps even reduced, time-frame.

REFERENCE LIST

1. Lee J, Miyazawa K, Tabuchi M, Kawaguchi M, Shibata M, Goto S. Midpalatal miniscrews and high-pull headgear for anteroposterior and vertical anchorage control: cephalometric comparisons of treatment changes. *Am J Orthod Dentofacial Orthop* 2013;**144**:238–250.
2. Suzuki EY, Suzuki B. Maxillary molar distalization with the indirect Palatal miniscrew for Anchorage and Distalization Appliance (iPANDA). *Orthodontics (Chic.)* 2013;**14**:e228–241.
3. Kim KB, Helmkamp ME. Miniscrew implant-supported rapid maxillary expansion. *J Clin Orthod* 2012;**46**:608–612.
4. Razavi MR. Molar intrusion using miniscrew palatal anchorage. *J Clin Orthod* 2012;**46**:493–498.
5. Kang YG, Kim JY, Nam JH. Control of maxillary dentition with 2 midpalatal orthodontic miniscrews. *Am J Orthod Dentofacial Orthop* 2011;**140**:879–885.
6. Deguchi T, Nasu M, Murakami K, Yabuuchi T, Kamioka H, Takano-Yamamoto T. Quantitative evaluation of cortical bone thickness with computed tomographic scanning for orthodontic implants. *Am J Orthod Dentofacial Orthop* 2006;**129**:721.e7–12.
7. Poggio PM, Incorvati C, Velo S, Carano A. "Safe zones": a guide for miniscrew positioning in the maxillary and mandibular arch. *Angle Orthod* 2006;**76**:191–197.
8. Choi JH, Yu HS, Lee KJ, Park YC. Three-dimensional evaluation of maxillary anterior alveolar bone for optimal placement of miniscrew implants. *Korean J Orthod* 2014;**44**:54–61.
9. Gracco A, Lombardo L, Cozzani M, Siciliani G. Quantitative cone-beam computed tomography evaluation of palatal bone thickness for orthodontic miniscrew placement. *Am J Orthod Dentofacial Orthop* 2008;**134**:361–369.
10. Winsauer H, Vlachojannis C, Bumann A, Vlachojannis J, Chrubasik S. Paramedian vertical palatal bone height for mini-implant insertion: a systematic review. *Eur J Orthod* 2014;**36**:541–549.
11. Ludwig B, Glasl B, Bowman SJ, Wilmes B, Kinzinger GS, Lisson JA. Anatomical guidelines for miniscrew insertion: palatal sites. *J Clin Orthod* 2011;**45**:433–441.
12. Maequezan M, Nojima LI, Ayres de Freitas AO, Baratieri C, Junior MA, Nojima M, et al. Tomographic mapping of the hard palate and overlying mucosa. *Braz Oral Res* 2012;**26**:36–42.
13. Kitai N, Yasuda Y, Takada K. A stent fabricated on a selectively colored stereo lithographic model for placement of orthodontic mini-implants. *Int J Adult Orthodon Orthognath Surg* 2002;**17**:264–266.
14. Miyazawa K, Kawaguchi M, Tabuchi M, Goto S. Accurate presurgical determination for self-drilling miniscrew implant placement using surgical guides and cone-beam computed tomography. *Eur J Orthod* 2010;**32**:735–740.
15. Kim SH, Choi YS, Hwang EH, Chung KR, Kook YA, Nelson G. Surgical positioning of orthodontic mini-implants with guides fabricated on models replicated with cone-beam computed tomography. *Am J Orthodon Dentofacial Orthop* 2007;**131**:S82–S89.
16. Liu H, Liu DX, Wang G, Wang CL, Zhao Z. Accuracy of surgical positioning of orthodontic miniscrews with a computer-aided design and manufacturing template. *Am J Orthod Dentofacial Orthop* 2010;**137**:728.e1–728.e10.
17. *Cone Beam CT for Dental and Maxillofacial Radiology. Evidence-Based Guidelines.* A report prepared by the SEDENTEXCT project. Available from http://www.sedentexct.eu/files/radiation_protection_172.pdf
18. Kim YJ, Lim SH, Gang SN. Comparison of cephalometric measurements and cone-beam computed tomography-based measurements of palatal bone thickness. *Am J Orthod Dentofacial Orthop* 2014;**145**:165–172.
19. Maino BG, Bednar J, Pagin P, Mura P. The spider screw for skeletal anchorage. *J Clin Orthod* 2003;**37**:90–97.
20. Maino BG, Mura P, Maino G, Paoletto E. Impianti palatini a scopo di ancoraggio ortodontico: metodica di precisione "MAPA" per la programmazione del sito implantare. *Mondo Ortodontico* 2004;**Feb**:97–106.
21. Liou EJ. Effective maxillary orthopedic protraction for growing Class III patients: a clinical application simulates distraction osteogenesis. *Prog Orthod* 2005;**6**:154–171.
22. Allegrini S, Paoletto E. Espansione e protrazione del mascellare in dentatura mista e permanente con tecnica di Liou modificata. 22. *Ortodonzia tecnica* 2009;**3**:7–13.
23. Schott TC, Ludwig B, Glasl BA, Lisson JA. A microsensor for monitoring removable-appliance wear. *J Clin Orthod* 2011;**45**:5181; Or
24. Schott TC, Goz G. Applicative characteristics of new microelectronic sensors Smart Retainer(R) and TheraMon(R) for measuring wear time. *J Orofac Orthop* 2010;**71**:339–347.
25. Ackerman MB, Thornton B. Posttreatment compliance with removable maxillary retention in a teenage population: a short-term randomized clinical trial. *Orthodontics (Chic.)* 2011;**12**:22–27.
26. Tsomos G, Ludwig B, Grossen J, Pazera P, Gkantidis N. Objective as-sessment of patient compliance with removable orthodontic appliances: a cross-sectional cohort study. *Angle Orthod* 2014;**84**:56–61.

doi:10.12889/2015_C00239